MAPPING URBAN GROWTH AND DEVELOPMENT AS CONTINUOUS FIELDS IN SPACE AND TIME

Christopher Small[1]

INTRODUCTION

Cities are often depicted as discrete entities – both on maps and in analysis. While the individual components of cities may be discrete (e.g. people, buildings, firms), the functional entity of a city can be difficult to define as a discrete object. Administrative boundaries of cities are discrete but in many ways they are functionally irrelevant to the processes that occur within the city and with its surrounding communities. Attempts to classify cities as discrete spatial objects generally fail to produce useful depictions because the definitions on which the classifications are based are often arbitrary. Two persistent obstacles to discrete classification of urban extent are the lack of a consistent definition and the scale dependence of the most easily measurable quantities (e.g land cover) on which the definitions are based.

As an alternative to discrete definition, cities can be depicted as parts of a continuum. Depiction of a city as part of a continuum can accommodate both form and function. In terms of form, a city might be considered a local maximum of density of some component, or combination of components (e.g. population density, building density, or road density) that varies continuously in space and time. In terms of function, a city might be considered a local maximum of activity, or combination of activities (e.g. economic output, innovation or information exchange).

Depicting cities as entities within continuous fields offers at least two advantages over discrete classification; flexibility and information content. Discrete classifications trade information for simplicity. The two modes of viewing geography in Google Earth (map & satellite) provide an example of this trade-off. The map view is generally simpler to interpret but it contains far less information than the satellite view. However, continuous fields can still provide a basis for discrete classification when

[1] Lamont Doherty Earth Observatory, Columbia University, Palisades, NY 10964 USA.

simplicity of depiction is needed. Continuous fields may be segmented into discrete components by imposing thresholds. For example, a city might be defined as the area with population density above some threshold. The ability to impose different thresholds on a single continuous field offers the flexibility to accommodate different definitions in situations where there is no consensus on a single definition. For example, a city might be considered alternately as a place with population density greater than 100 persons/km^2, 1000 persons/km^2 or 10,000 persons/km^2. One important asymmetry between discrete and continuous depictions is the ability of continuous fields to represent abrupt changes and boundaries and the inability of discrete depictions to represent gradual changes and gradients.

The objective of this paper is to illustrate some benefits of continuous fields for depiction of urban growth and development. In this context, urban growth refers to expansion in space, either vertical or horizontal. Development refers to progressive changes in form or function that lead to improved living standards. Continuous field depictions are illustrated using remotely sensed imagery – but the underlying concepts are generally applicable to other measurable quantities like population density or economic activity. Continuous field depictions can be extended to represent change by mapping differences in time. Examples are provided for multiple quantities (land cover type and night light brightness), measured by multiple sensors (Landsat, DMSP-OLS and VIIRS) at multiple times (1990, 2010, 2012). Some characteristics of urban growth and development are illustrated with continuous field depictions of large cities and their surrounding regions from the rapidly developing BRIC countries; Brazil, Russia, India and China. In addition to multi-scale, multi-sensor, multi-temporal depictions of urban areas as continuous fields, the utility of discretization with multiple thresholds is illustrated by comparing city size distributions obtained from night lights.

The Land Cover Continuum

Land cover can be represented as continuous fields of constituent components at some spatial scale. This is analogous to common measures of density (population, road, building). Continuous fields of land cover components are especially convenient because they accommodate the fixed spatial scale imposed by the Instantaneous Field Of View (IFOV) of sensors commonly used to map land cover. Areal abundance of land cover components (e.g. trees, water, soil) at the scale of individual pixels provides a convenient, and easily measurable, basis for representing a variety of land cover types (e.g. forest, agriculture, wetland) from which land use may be inferred. Continuous fields of land cover can be derived from multispectral measurements of land surface reflectance by optical sensors because the mixed radiance field within the sensor's IFOV can often be "unmixed" to provide accurate estimates of the areal abundance of the spectral endmembers of different land cover components (Adams and Gillespie 2006; Adams et al. 1986). In this study, a standardized spectral mixture model (Small and Milesi 2013) is used to estimate the areal abundance of Substrates (rock, soil, impervious), Vegetation and Dark components (water, shadow, absorptive materials) from Landsat imagery. An important benefit of the Substrate Vegetation Dark (SVD) model of land cover is its linearity of scaling in a wide range of environments. The SVD spectral endmembers have been shown to scale linearly in area from 2 m up to 30 m scales (Small and Milesi 2013). Because endmember fractions represent the fractional area of a pixel occupied by each endmember, the continuous fields of endmember abundance can represent both abrupt changes and gradients over a range of scales. Applying the linear spectral mixture model to reflectance imagery collected by intercalibrated sensors on board the Landsat satellites provides self-consistent observations of cities and their surroundings and how they have changed since the early 1980s. This provides a baseline for quantifying changes at spatial scales and resolutions that can inform our understanding of the processes driving the changes.

Although cities are often easily recognized in Landsat imagery, discrete classifications of urban land cover are notoriously inaccurate (Yu et al. 2014). This is a simple result of the fact that urban land cover heterogeneity violates the cardinal assumption of spectral homogeneity on which all discrete classifiers rely. The root of the problem is the spectral non-uniqueness of urban land cover, in which many of the materials found in the urban environment are spectrally indistinguishable from materials found in non-urban environments. The most common source of error in classifications of urban land cover is the spectral ambiguity between pervious and impervious substrates. However, we find a partial solution to this problem in considering the temporal variability of pervious and impervious substrates. The most common impervious substrate, soil, differs from impervious substrates primarily in its retention of moisture. Soils absorb moisture but, by definition, impervious surfaces do not. All but the most hydrophobic soils absorb water rapidly and dehydrate relatively slowly. The commonly observed phenomenon of moisture darkening causes soil reflectance to change continuously with moisture content. In contrast, impervious surfaces tend to dry quickly therefore maintaining a more consistent reflectance when imaged by satellite based sensors.

Urban land cover can be distinguished more effectively when temporal variability (or consistency) of reflectance is considered. Pervious and impervious substrates can be distinguished more easily because the reflectance of impervious surfaces does not vary with moisture content or vegetation abundance as pervious soils do. In addition, the presence of persistent building shadow in urban environments can distinguish stable mixtures of impervious surface (Substrate) and shadow (Dark) from time-varying reflectance of soils of different moisture content. To exploit this difference we use Landsat imagery acquired in different seasons of the same year and compute the temporal mean and standard deviation of each SVD component. Each mean fraction provides information about the subpixel components of land cover while the standard deviation provides information on the seasonal variability of the land cover. Both the mean and standard deviation vary continuously – as do the endmember fractions. In this paper, land cover is depicted as Red, Green, Blue (RGB) composites of mean Substrate, Vegetation and Dark fractions (Fig. 1).

Changes in land cover (urban or otherwise) can be represented continuously as changes in endmember fractions with time. This allows us to avoid (or at least postpone) the loss of information inherent in discrete classification. Changes in land cover can be depicted at least as accurately, and more informatively, as continuous changes in SVD components at subpixel scales. These changes can be visualized as direct comparisons of SVD composites for different time periods, or as tri-temporal changes of each component separately (Fig. 1). By combining continuous fields of the same quantity at different times as an RGB color composite, unchanged pixels with equal RGB components through time appear shades of gray while any change appears as a color.

The Continuum of Development

Development is not a discrete process. By any measure, there are varying levels of development spanning a wide range for different places at different times. Night light brightness, also measured by sensors aboard satellites, provides a complementary global proxy for development. The Defense Meteorological Satellite Program Operational Line Scanner (DMSP OLS) has been imaging night lights since the early 1970s (Croft 1973). The more recent digital data have been used to produce annual global composites of temporally stable nighttime lights from 1992 to 2008 (Elvidge et al. 2001). The Earth Observation Group at NOAA NGDC has developed procedures to make cloud-free annual composites of the nighttime visible band DMSP-OLS data (Elvidge et al. 2001). The result is a set of composite images in which each 30 arc second (~1 km at the equator) pixel gives the annual average brightness level in units of 6 bit digital numbers (DN) spanning the range 0 to 63. Additional procedures are used to remove ephemeral lights (mostly fires) and background noise to produce gridded stable lights products. The data are available for download from: http://www.ngdc.noaa.gov/dmsp/downloadV4composites.html (access 29 June, 2014).

Night lights are known to overestimate the spatial extent of development at the periphery of settlements (Elvidge et al. 1997). In a comparison of Landsat and night lights for 16 cities worldwide, (Small et al. 2005) showed that differences in urban form and intensity of lighting preclude the use of a single threshold for all cities and that thresholding at the high levels results in the complete attenuation of large numbers of smaller settlements. Comparisons of stable light with 30 m resolution Landsat imagery on a wide variety of population density gradients indicates that average brightness increases with increasing spatial density of impervious substrate reflectance and shadow associated with constructed surfaces (Small et al, 2005) as well as actual maps of impervious surfaces (Elvidge et al, 2007). Comparisons with land cover maps illustrate the spatial correspondence of dim lights (DN < ~12) with agricultural and low population density land use while average brightness increases with both settlement size and intensity of development along urban-rural gradients. The spatial extent of the overglow is usually greater than the extent of high density impervious surface but it does not generally extend into areas that are completely undeveloped – except for short distances along coastlines. Comparisons with higher resolution images (see: www.LDEO.columbia.edu/~small/LandCoverLight) indicate that the dimly lit areas with DN < ~12 almost always contain some indication of anthropogenic land cover (e.g. agriculture), even when not coincident with high spatial densities of impervious surface typically associated with urban development.

To the extent that brightness of night light is indicative of the level of development (economic or infrastructural) of an area, changes in urban development can be inferred from changes in night light brightness. Combining annual mean night light brightness for different years in the RGB channels of a color image depicts change as color. Unchanged pixels will have approximately equal brightness values at each time to yield shades of gray as equal fractions of red, green and blue (Figure 1). Any change of pixel brightness between the years of the composite appears as a color. The implicit assumption is that the processes responsible for the overglow do not change in time so that changes in brightness (direct or overglow) are in response to actual changes in the number or brightness of light sources with time. In a multitemporal comparison of changes in night light from OLS and changes in land cover from Landsat, (Small and Elvidge 2013) found consistent agreement between increases in substrate-shadow mixtures related to built environments and increases in night light brightness within and around large cities in Asia.

We find a partial solution to the problem of night light overglow by combining tri-temporal RGB composites of OLS night lights with a higher spatial resolution night light measurements collected by the day night band (dnb) of the VIIRS sensor on board the NASA/NOAA Suomi satellite. Because the hue of the tri-temporal composite represents the change and the lightness represents the mean brightness, we can separate these two components using a cylindrical color transform like Hue Saturation Value (HSV) or Hue Lightness Saturation (HLS). Once the brightness component is separated from the change component, the OLS brightness (including overglow) can be replaced with the more detailed VIIRS brightness and the inverse color transform can be applied to return to RGB color space. The resulting composite is much more spatially detailed (comparable to VIIRS) but depicts decadal changes in brightness as color. This image fusion process, and the results, are illustrated in Figure 2.

Comparisons of Urban Form and Evolution

The complementarity of continuous field depictions of urban land cover and night light brightness are illustrated in four comparisons of urban systems and their surrounding communities and environments. São Paulo, Moscow, New Delhi and Beijing represent the apex of the urban systems for the large and rapidly developing economies of Brasil, Russia, India and China. The multi-scale, multi-sensor, multi-temporal comparisons in Figures 3, 4, 5 and 6 illustrate several important similarities and differences among these systems that would be difficult or impossible to represent accurately with discrete depictions.

The process of spectral darkening observed in built and lighted areas around the periphery of São Paulo is an inherently continuous process resulting from increases in dark fraction below the scale of the pixel. This can be explained physically as an increase in the area in shadow as building heights increase and infill development increases shadow fraction in previously illuminated areas. This process occurs in more recently built up areas around the periphery of São Paulo but also within the older parts of the city where high rise development has occurred over the past two decades.

Darkening from low rise development also occurs on the periphery of New Delhi – but is not observed in the more rapid growth of Beijing or the more stable land cover around Moscow. This kind of information on the changing composition of urban land cover would be lost in a discrete classification.

Quantifying the Structure of Continuous Fields

Continuous fields and discrete classifications are not mutually exclusive. In fact, discrete classifications are often derived from continuous fields. The most common examples are supervised land cover classifications of multispectral imagery. In the case of supervised classification, training samples are selected for each class and the moments of the statistical distributions of the samples are used to derive decision boundaries upon which the classifications are based. However, this approach assumes that each class has unique, non-intersecting distributions. This assumption is violated in the case of different land cover classes with similar or indistinguishable spectral properties. To make matters worse, even accurate classifications are often non-repeatable without knowledge of the specific training samples used. Since the general spectral properties of land cover classes are rarely reported in studies using supervised classification, and sensitivity to selection of training samples is rarely discussed, the uniqueness of the classification cannot be determined. Fortunately, the process of discretizing a continuous field need not suffer from these shortcomings. Simpler approaches are often possible.

The spatial structure and characteristics of continuous fields can be quantified by the process of segmentation. Applying a threshold to a continuous field produces discrete segments of the areas where the value of the field exceeds the threshold. Different thresholds produce different distributions of segments. A simple example is given by successive thresholding of night light brightness. Given the presence of overglow and varying definitions of urban extent, it is not clear what level of brightness best represents an appropriate measure of development for a specific application. Rather than choosing a single brightness threshold based on arbitrary or ad hoc criteria, a set of successive thresholds can be applied to the night light brightness field to determine the sensitivity of the resulting discrete maps to the threshold chosen. This is illustrated in Figure 7. The results of the segmentation process can be represented by the size distribution of the areas of the discrete segments that result from each threshold. The effect of different thresholds is reflected in changes in the resulting segment size distributions.

The approach of successive thresholding is applied to the 2012 VIIRS dnb night light imagery. The imagery is divided into three non-overlapping longitudinal sectors referred to as western (North and South America), central (Europe, Africa, Middle East) and eastern (Asia). The dividing longitudes are chosen to avoid breaking any spatially contiguous lighted areas. For each sector, four different brightness thresholds are applied to the Log_{10} of brightness and the size distribution of spatially continuous lighted areas are calculated. The lower threshold of 1 radiance unit is selected at the noise floor where background luminance is comparable to the dimmest anthropogenic lights. The upper threshold of 10 radiance units is chosen at the level where the smallest anthropogenic lights begin to be completely attenuated. The rank-size distributions of the segments resulting from these thresholds are shown in Figure 8.

For each threshold the size distribution of segments spans several orders of magnitude in area. These types of "heavy tailed" Pareto distributions are often represented with power laws of the form

$$N = Ax^{-\alpha}$$

where the number of objects, N, larger than some size, X, follows is determined by the exponent α and a constant A. The exponent represents the slope of the distribution when the Log_{10} of the size of each object is plotted against the Log_{10} of its ordinal rank (largest to smallest). The physical meaning of the exponent, or slope of the distribution, is related to total area of objects of different sizes. Larger negative exponents correspond to distributions in which large objects account for more total area than small objects.

Smaller negative exponents correspond to the opposite case where small objects account for more total area than large objects. A distribution with an exponent of -1 corresponds to the transitional case of a uniform size distribution in which objects of each size range account for the same total area. In the case of segment areas, the slope of the rank-size distribution, given by the exponent of the best fit power law, indicates whether larger segments account for more or less total area than smaller segments.

In the case of the size distribution of night lights, different brightness thresholds produce very similar segment size distributions. For each rank-size distribution of segment sizes, a power law was fit using the method of (Clauset et al. 2009). The rank-size distributions and the best fit exponents of the corresponding power laws are shown in Figure 8. Despite the order of magnitude difference in brightness thresholds, the shapes of the resulting rank-size distributions are very similar with nearly identical exponents for the best fit power law of each. The most obvious effect of increasing the brightness threshold is to reduce both the size and number of segments. However, the slope is not sensitive to the brightness threshold. This result holds for each of the three longitudinal sectors and for the global distributions. This implies that the brightness thresholds produce very similar distributions with nearly equal total areas of segments of all sizes. However, the largest segments are much larger than individual cities. They represent vast spatial networks of interconnected development.

The same approach of discrete segmentation of night light brightness fields can inform our understanding of how urban systems evolve with time. Figure 9 shows the rank-size distributions obtained by (Small and Elvidge 2013) for China, India and all of Asia between 1992 and 2009. Although all of the rank size distributions are well fit by power laws with exponents very close to -1, the shapes of the upper tails of the distributions are different for China and India. This reflects real differences in the spatial structure and size distributions of the urban systems in these two countries.

The process of segmenting night lights at increasing brightness thresholds provides information on the spatial structure of the brightness field and, by inference, the spatial structure of the light sources responsible for it. As the threshold is increased the dimmer peripheral lights connecting the brighter urban cores are attenuated - causing the larger networks to fragment into smaller subnets. Increasing the threshold also attenuates the dimmer pixels at the periphery of smaller isolated light sources causing them to shrink in area. Both fragmentation and shrinkage result in movement of lighted segments downward through the rank-size distribution. Despite the continuous reordering of the distribution as segments shrink and migrate downward, the slope of the distribution remains close to -1. The reverse of this process, decreasing the threshold, is analogous to the urban growth process. Peripheral growth of small settlements causes them to move up through the distribution discontinuously at different rates. Spatial coalescence of settlements of all sizes causes newly joined settlement networks to move upward through the distribution at varying rates determined by the spatial distribution of light sources of different sizes. Even though the brightness field is continuous, the process of successive segmentation can produce discontinuous results with abrupt changes occurring when two or more segments become connected into a single larger segment. As a result, the size distribution of segments produced by one threshold can be very different from the size distribution of segments from a slightly different threshold.

The segment size distribution of lighted areas has a direct relevance to fundamental questions of urban growth and development. Imposing a threshold on a continuous field of night light brightness produces a binary map of lighted areas against an unlighted background. This is analogous to, but different from, city size distributions based on population residing within administrative units. If areas with night light brightness above a certain threshold are considered to be urban, segmentation of a brightness map with a single threshold produces one possible depiction of urban extent. In the absence of a single such threshold, it is possible to choose multiple thresholds to see how the resulting distributions change.

Urban Growth and Spatial Networks of Development

City size distributions, defined on the basis of population, are often described as power laws. Auerbach (Auerbach 1913) made the initial observation that the product of city population and ordinal rank was approximately constant for Germany. Lotka (Lotka 1941) subsequently reported a hyperbolic rank-size relationship for U.S. city populations, noting that the slope of the Log_{10} rank-size plot was not exactly -1 but -0.93 with some of the larger cities being smaller than predicted. Zipf later estimated that the exponent of the power law is also close to -1 for U.S. cities (Zipf 1942), a finding that holds for the frequency of usage of words, sizes of firms, and several other socioeconomic variables (Zipf 1949). He postulated a universal principal of least effort from which the power law emerges as an optimal distribution for a variety of processes. The special case of a power law distribution with an exponent of -1 is often referred to as Zipf's Law; it has been tested repeatedly for cities, yielding mixed but generally consistent results (Gabaix et al. 2004; Nitsch 2005; Pumain 2004; Soo 2005). The consistency of Zipf's Law has attracted sustained interest for several decades, and been the basis for a multitude of models (Berry and Garrison 1958; Gabaix 1999; Lotka 1941; Pumain 2006) , but the varying degree and extent of agreement with observation seem to preclude consensus on either the universality of the law (Gan et al. 2006; Soo 2005) or its underlying causes (Batty 2006a, b; Lotka 1941; Pumain 2004, 2006). On empirical grounds alone, the assertion of a universal power law for city size remains controversial because the estimates of linearity and slope of the power law rank-size distribution often vary over time and among countries (Gabaix et al. 2004; Nitsch 2005; Pumain and Moriconi-Ebrard 1997; Soo 2005). However, these irregularities may be the result of the way population is measured. Census enumerations are tied to administrative units. These administrative units may be appropriate for smaller isolated cities but they impose artificial boundaries on cities embedded within larger metropolitan areas. The administrative fragmentation of large agglomerations limits the size of population that can be represented and precludes the consideration of larger agglomerations in the analysis. Using a more accurate and consistent spatial depiction of urban areas could avoid some of these shortcomings and potentially resolve the controversy over Zipf's Law.

The rank-size distributions of spatially contiguous lighted segments are consistent with power law distributions with exponents of -1, regardless which brightness threshold is applied within an order of magnitude of range. This observation complements previous analyses of city size distribution based on population – but extends it into the spatial dimension. The fact that the largest contiguous lighted segments correspond to spatial networks much larger than individual cities suggests that the regularity of these distributions may be fundamentally related to their spatial structure and the process of urban growth and spatial coalescence of individual settlements into network structures.

A detailed discussion is beyond the scope of this paper but the result illustrates the power of the continuous field representation of urban environments and land cover. Treating night light brightness as a proxy for urban development allows for self-consistent mapping at global scales – as well as direct comparison to continuous fields of land cover abundance derived from Landsat observations. Together, these two continuous field depictions of urban environments allow for retrospective analyses of urban extent – without relying on ad hoc or arbitrary definitions of what defines urban.

Depiction of urban areas with continuous fields can be extended to the concept of a continuum of urban form and function. Taking land cover, and by implication land use, as a relatively simple example, the continuum of urban form could extend from completely constructed anthropogenic environments composed only of buildings and streets to a completely natural environment with no anthropogenic modifications. At present, discrete land cover maps attempt to represent this structure – but are limited by the scale dependence and accuracy of the classification procedure. A continuous field of land cover could provide a viable alternative to the discrete representation for many applications. Taking population density as a relatively simple example, the continuum of urban function could extend from very densely populated areas with large numbers of people engaged in a common activity (e.g. a sports arena filled with spectators) to very sparsely populated areas where little or no human activity occurs. At present, discrete census enumerations attempt to represent this structure – but are limited by the spatial resolution of the census administrative units and the fact that census enumerations measure where people sleep, not where they work. A continuous field of ambient population density, derived from a disaggregation of census data with continuous fields of night light brightness and land cover fractions, could provide a probability density distribution that accounts for the mobility of population and the uncertainty in its measurement. As illustrated here, a single continuous field representation can be segmented as necessary to suit the specific needs of different applications.

ACKNOWLEDGEMENTS

This research was funded most recently by the NASA Land Cover and Land Use Change Program (grant LCLUC09-1-0023) and Interdisciplinary Science Program (grants NNX12AM89G & NNN13D876T). The idea of continuous fields of urban land cover and development evolved from years of discussions with Deborah Balk, Ligia Barrozo, Uwe Deichmann, Chris Elvidge, Valentina Mara, Cristina Milesi, Mark Montgomery, Reinaldo Peréz-Machado, Francesca Pozzi and Greg Yetman.

REFERENCES

Adams, J.B., & Gillespie, A.R. (2006). *Remote Sensing of Landscapes with Spectral Images*. Cambridge, UK: Cambridge University Press Adams, J.B., Smith, M.O., & Johnson, P.E. (1986). Spectral mixture modeling; A new analysis of rock and soil types at the Viking Lander 1 site. *Journal of Geophysical Research, 91*, 8098-8122

Auerbach, F. (1913). Das Gesetz der Bevolkerungskonzentration. *Petermanns Geographische Mitteilungen, 59*, 74-76 Batty, M. (2006a). Heirarchy in cities and city systems. In D. Pumain (Ed.), *Hierarchy in natural and social sciences* (pp. 143-168). Dordrecht Germany: Kluwer Batty, M. (2006b). Hierarchy in cities and city systems. In D. Pumain (Ed.), *Hierarchy in Natural and Social Sciences* (pp. 143-168): Springer Berry, B.J.L., & Garrison, W.L. (1958). Alternate explanations of urban rank-size relationships. *Annals of the Association of American Geographers, 1*, 83-91

Clauset, A., Shalizi, C.R., & Newman, M.E.J. (2009). Power-law distributions in empirical data. *SIAM Review, 51*, 661-703

Croft, T.A. (1973). Night-time Images of the Earth From Space. *Scientific American, 239*, 68-79

Elvidge, C.D., Baugh, K.E., Kihn, E.A., Kroehl, H.W., & Davis, E.R. (1997). Mapping city lights with nighttime data from the DMSP operational linescan system. *Photogrammetric Engineering and Remote Sensing, 63*, 727-734

Elvidge, C.D., Imhoff, M.L., Baugh, K.E., Hobson, V.R., Nelson, I., Safran, J., Dietz, J.B., & Tuttle, B.T. (2001). Night-time lights of the world: 1994-1995. *Isprs Journal of Photogrammetry and Remote Sensing, 56*, 81-99

Gabaix, X. (1999). Zipf's law for cities: an explanation. *Quarterly Journal of Economics 114*, 739–767

Gabaix, X., Ioannides, Y.M., Henderson, J.V., & Jacques-FranÁois, T. (2004). Chapter 53 The evolution of city size distributions. *Handbook of Regional and Urban Economics* (pp. 2341-2378): Elsevier Gan, L., Li, D., & Song, S. (2006). Is the Zipf law spurious in explaining city-size distributions? *Economics Letters, 92*, 256-262

Lotka, A. (1941). The law of urban concentration. *Science, 94*, 164

Nitsch, V. (2005). Zipf zipped. *Journal of Urban Economics, 57*, 86-100

Pumain, D. (2004). Scaling laws and urban systems. In (p. 26). Santa Fe NM: Santa Fe Institute Pumain, D. (2006). Alternative explanations of heirarchical differentiation in urban systems. In D. Pumain (Ed.), *Hierarchy in natural and social sciences* (pp. 169-222). Dordrecht Germany: Kluwer Pumain, D., & Moriconi-Ebrard, F. (1997). City Size distributions and metropolisation. *Geojournal, 43*, 307-314

Small, C., & Elvidge, C.D. (2013). Night on Earth: Mapping decadal changes of anthropogenic night light in Asia. *International Journal of Applied Earth Observation and Geoinformation, 22*, 40-52

Small, C., & Milesi, C. (2013). Multi-scale Standardized Spectral Mixture Models. *Remote Sensing of Environment, 136*, 442-454

Small, C., Pozzi, F., & Elvidge, C.D. (2005). Spatial Analysis of Global Urban Extent from DMSP-OLS Night Lights. *Remote Sensing of Environment, 96*, 277-291

Soo, K.T. (2005). Zipf's Law for cities: a cross-country investigation. *Regional Science and Urban Economics, 35*, 239-263

Yu, L., Liang, L., Wang, J., Zhao, Y., Cheng, Q., Hu, L., Liu, S., Yu, L., Wang, X., Zhu, P., Li, X., Xu, Y., Li, C., Fu, W., Li, X., Li, W., Liu, C., Cong, N., Zhang, H., Sun, F., Bi, X., Xin, Q., Li, D., Yan, D., Zhu, Z., Goodchild, M.F., & Gong, P. (2014). Meta- discoveries from a synthesis of satellite-based land-cover mapping research. *International Journal of Remote Sensing*, 4573-4588

Zipf, G.K. (1942). The Unity of Nature, Least-Action, and Natural Social Science. *Sociometry, 5*, 48-62

Zipf, G.K. (1949). *Human Behavior and the Principle of Least-Effort*: Addison Wesley

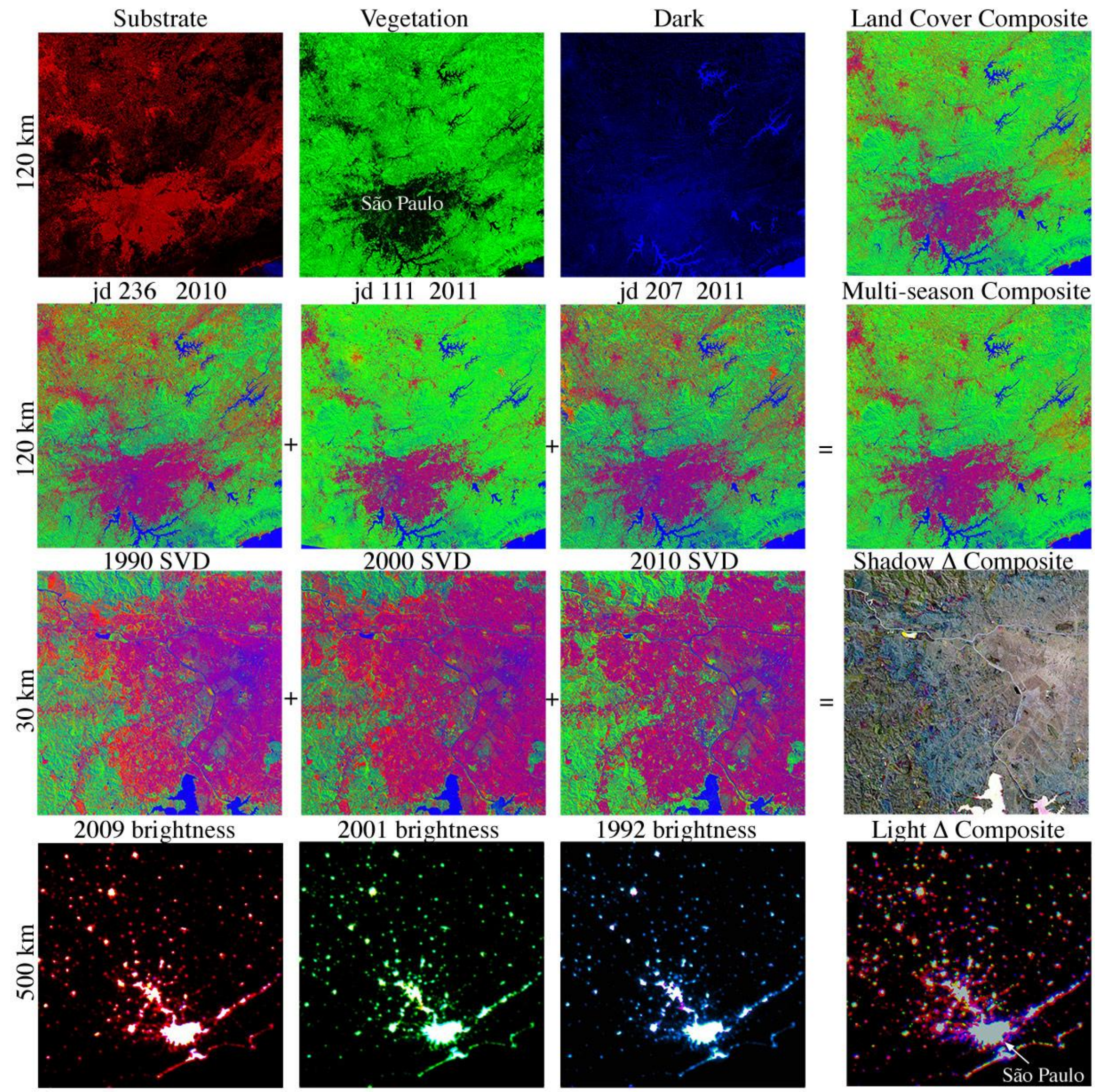

Figure 1 Complementary applications of continuous field color composites of São Paulo. *Land Cover Composite* (top row); Diversity of land cover at subpixel scales can be represented as RGB composites of Substrates (rock, soil, impervious), Vegetation (trees, grasses, agriculture) and Darks (shadow, water). SVD endmember fractions can be estimated with Landsat multispectral imagery from the mid-1980s to present. *Multi-season Composite* (upper middle row); Seasonal variability of reflectance and illumination can highlight different types of land cover in multi-season averages of SVD fractions. Soils are distinguished from impervious substrates by greater variability resulting from seasonal variations in moisture and vegetation cover. Temporally stable impervious substrates in urban areas (red) are mixed with persistent building shadow (blue) at the scale of Landsat's 30m pixel. *Shadow Change Composite* (lower middle row); Increasing shadow fraction in peri-urban municipalities of São Paulo over the past two decades is depicted in SVD composites as a progressive change from red to magenta. The shadow change composite (*R*: D_{1990} *G*: D_{2000} *B*: D_{2010}) clearly shows a blue halo in the peri-urban areas and isolated patches of blue within the urban core where high rise construction has occured since 1990. *Night Light Change Composite* (bottom row); Changes in areal extent and brightness of DMSP-OLS night light are depicted as color) while unchanged areas are shades of gray. White areas indicate saturation of the OLS sensor where changes in urban core lighting cannot be detected. The urban perimeter and most small settlements are red or yellow suggesting increased brightness since 1992.

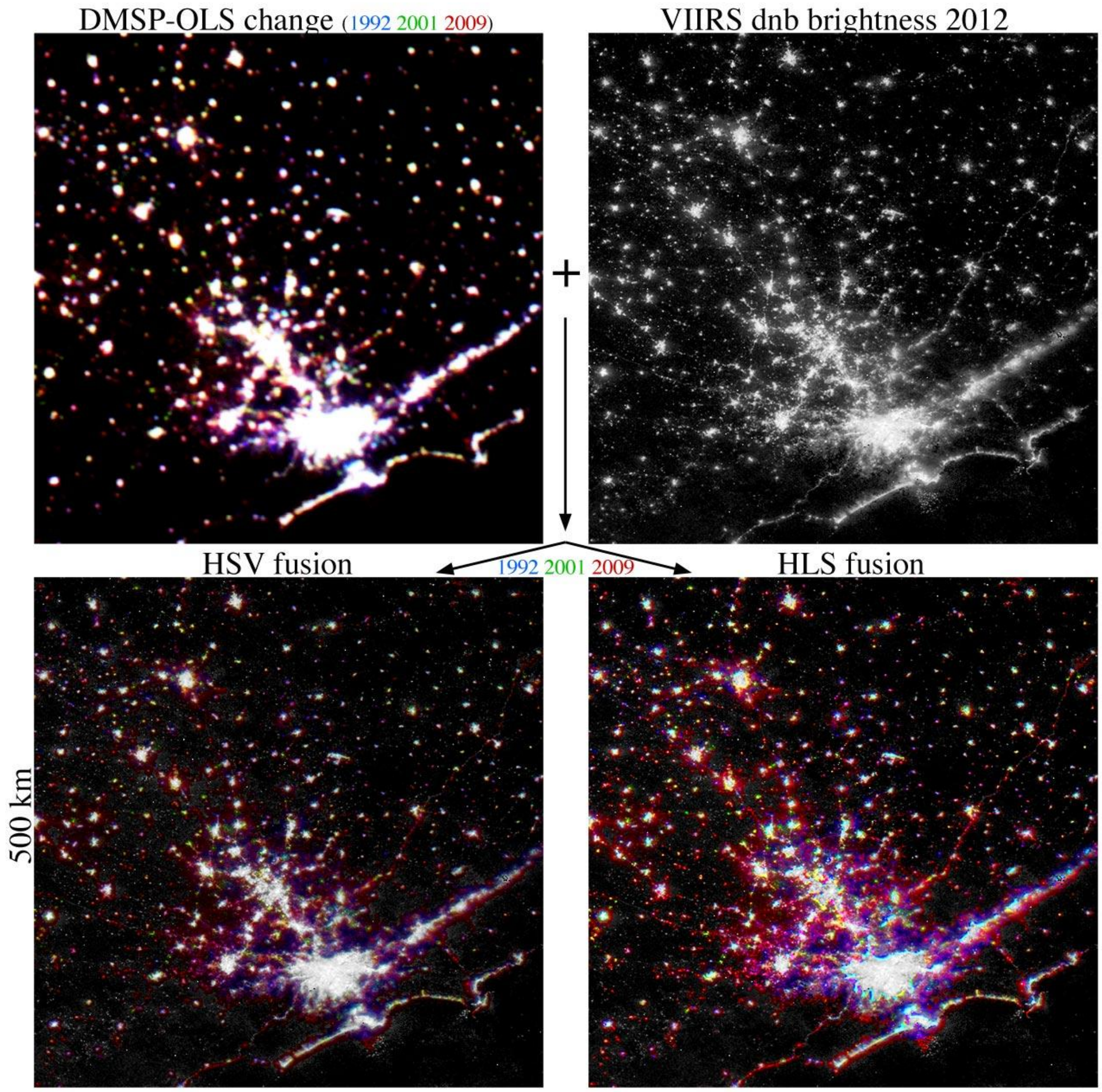

Figure 2 Tri-temporal night light fusion process illustrated for São Paulo and surrounding area. Tri-temporal (TT) composite of OLS shows changes in annual brightness as colors. VIIRS dnb shows much more detailed night light luminance at higher spatial resolution, spanning a wider range of brightnesses without saturation in bright urban cores. Transforming TT RGB to a cylindrical color space (either HLS or HSV) separates the change component (Hue) from the brightness component (Lightness or Value). Replacing the stable OLS brightness with the 2012 VIIRS brighntess and inverse transforming back to RGB space drastically reduces overglow and shows both change areas (color) and unchanged lights (gray) in much greater detail than the OLS TT image. Perceptually, the HLS fusion emphasizes changes making it easier to see patterns in smaller lights that have changed over the previous 20 years - but both enhancements show the same spatial and change patterns. While most smaller settlements show pronounced increases in luminance, either during the 1990s (yellow) or post-2000 (red), some peripheral areas of larger settlements (notably São Paulo) show some apparent decreasse in brightness post-2000 (cyan). However, symmetric yellow-cyan bands at periphery of intermediate size lights likely result from systematic shifts between different year composites. Very bright isolated pixels detected by VIIRS are artifacts - not cities. These may be related to the South Atlantic Anomaly, a phenomenon resulting from a deflection of the Van Allen belt in this region offshore southern Brazil.

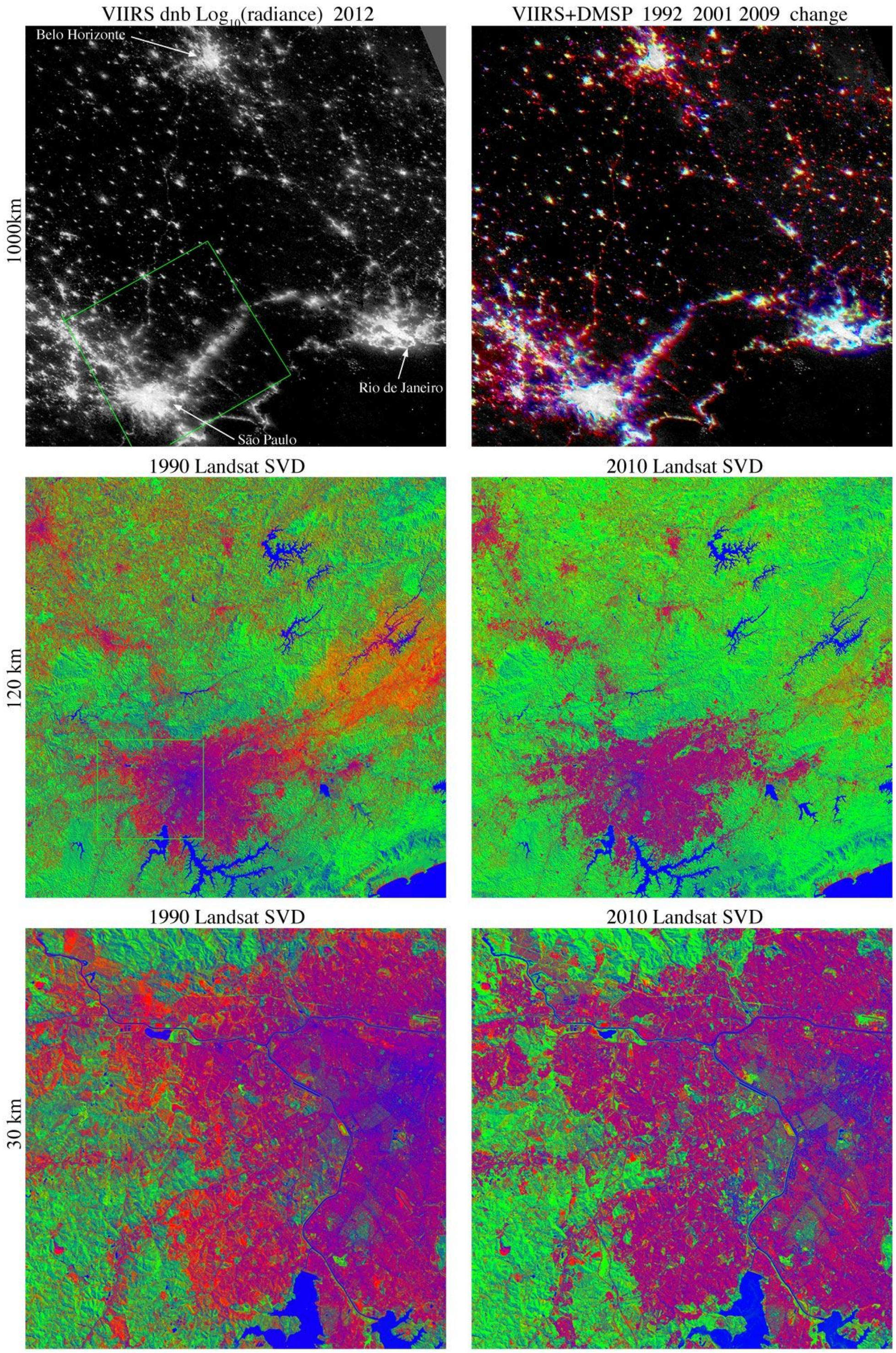

Figure 3 Decadal change of land cover and night light in and near São Paulo. Chaotic patterns of change in night light brightness for segments of all sizes show net brightening of all but the largest agglomerations since 1992. A relative scarcity of peripheral brightening of larger agglomerations suggests that whatever growth has occurred has not resulted in great increases in developed land area. This is supported by a relative scarcity of places where vegetation has been replaced by substrate+shadow mixtures in the Landsat reflectance.Increasing dark endmember fraction around the periphery of São Paulo suggests increased shadow in previously developed areas with high substrate fractions in 1990. Increase in shadow is consistent with vertical growth and infilling development. In addition to darkening of peripheral areas, numerous smaller areas throughout the urban core show moderate shadow fractions increasing substantially as a result of high rise development.

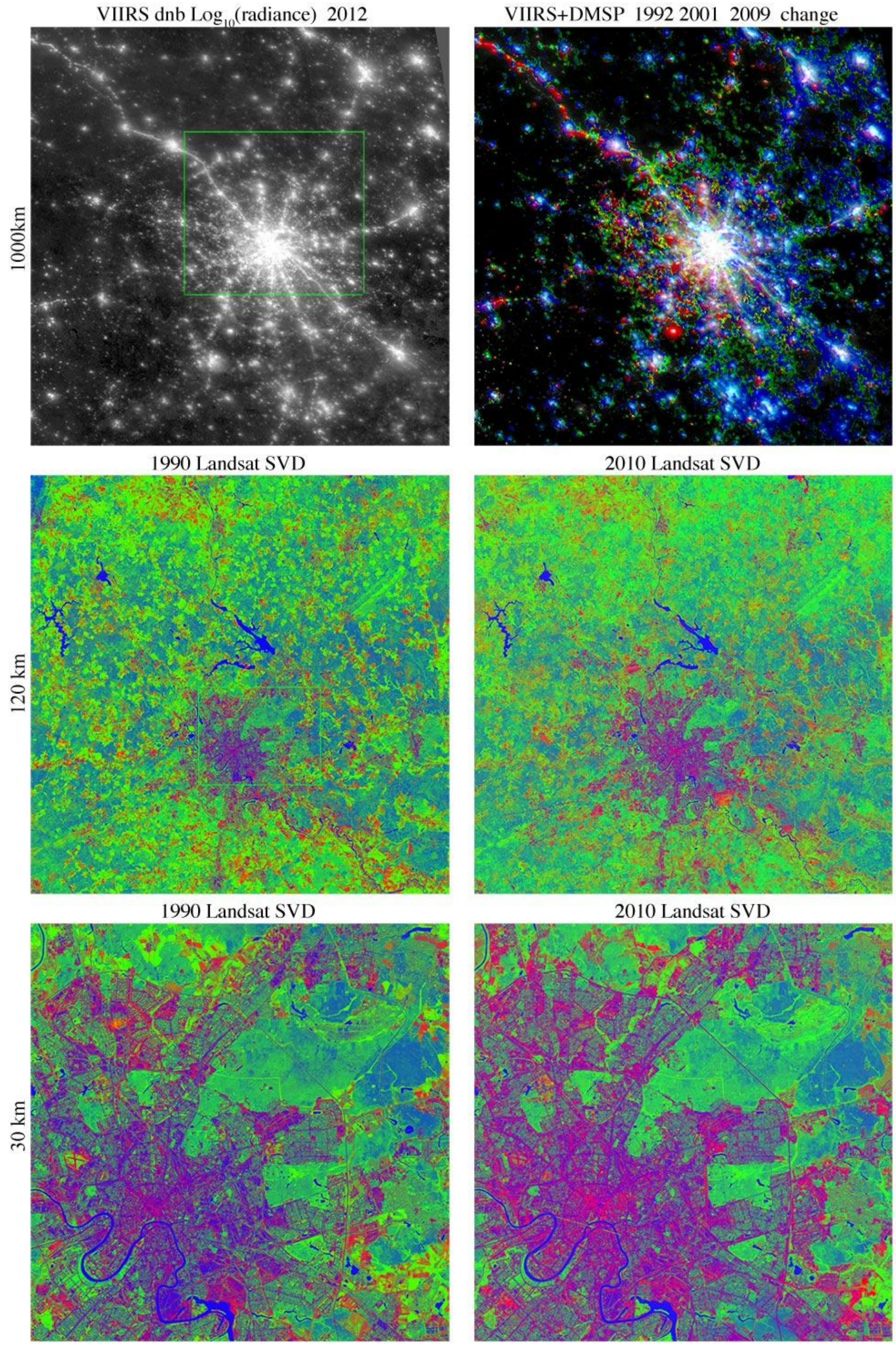

Figure 4 Decadal change of land cover and night light in and near Moscow. Change in night lights indicates brightening (red, yellow) on the immediate periphery of the city with dimming (blue, green) in surrounding areas. The prominent exception is the increased brightness along the road to St. Petersburg to the northwest. Change of Landsat SVD fractions over the same time period shows both extensive (expansion) and intensive (infilling) development as increases in the area of substrate (red) + shadow (blue) reflectance replacing both forest (green) and fallow agricultural fields (red). These changes are not seen further from the urban center.

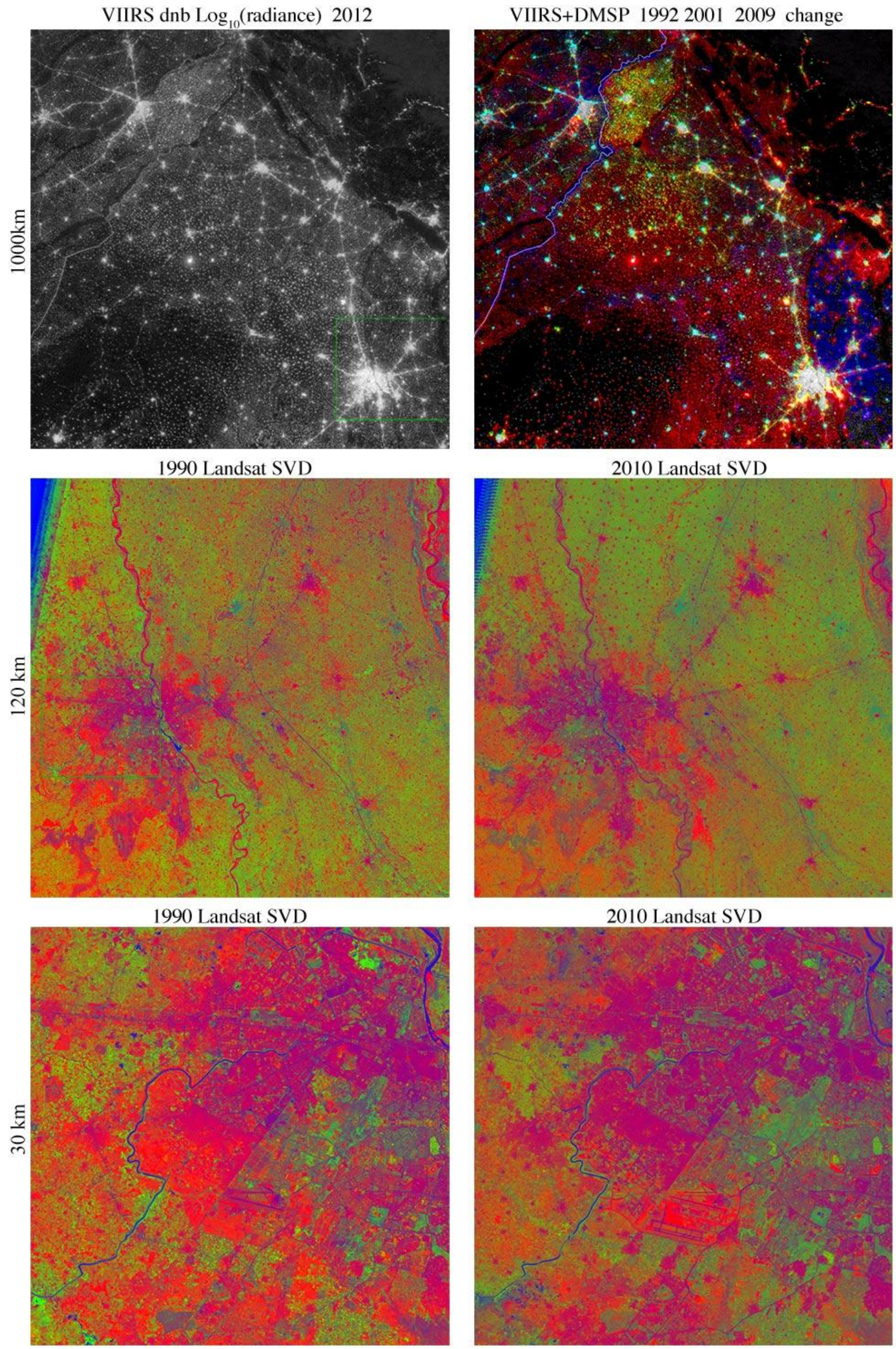

Figure 5 Decadal change of land cover and night light in and near New Delhi. Complex patterns of change in night lights correspond to administrative boundaries. The India-Pakistan border is clearly visible as a continuous lighted band separating contrasts in background luminance level and change. State boundaries within India are also clearly visible as different changes in background luminance. Change in Landsat SVD fractions are consistent with extensive and internsive growth of settlements of all sizes throughout the region. The most pronounced changes are seen at the periphery of New Delhi and the larger surrounding cities.

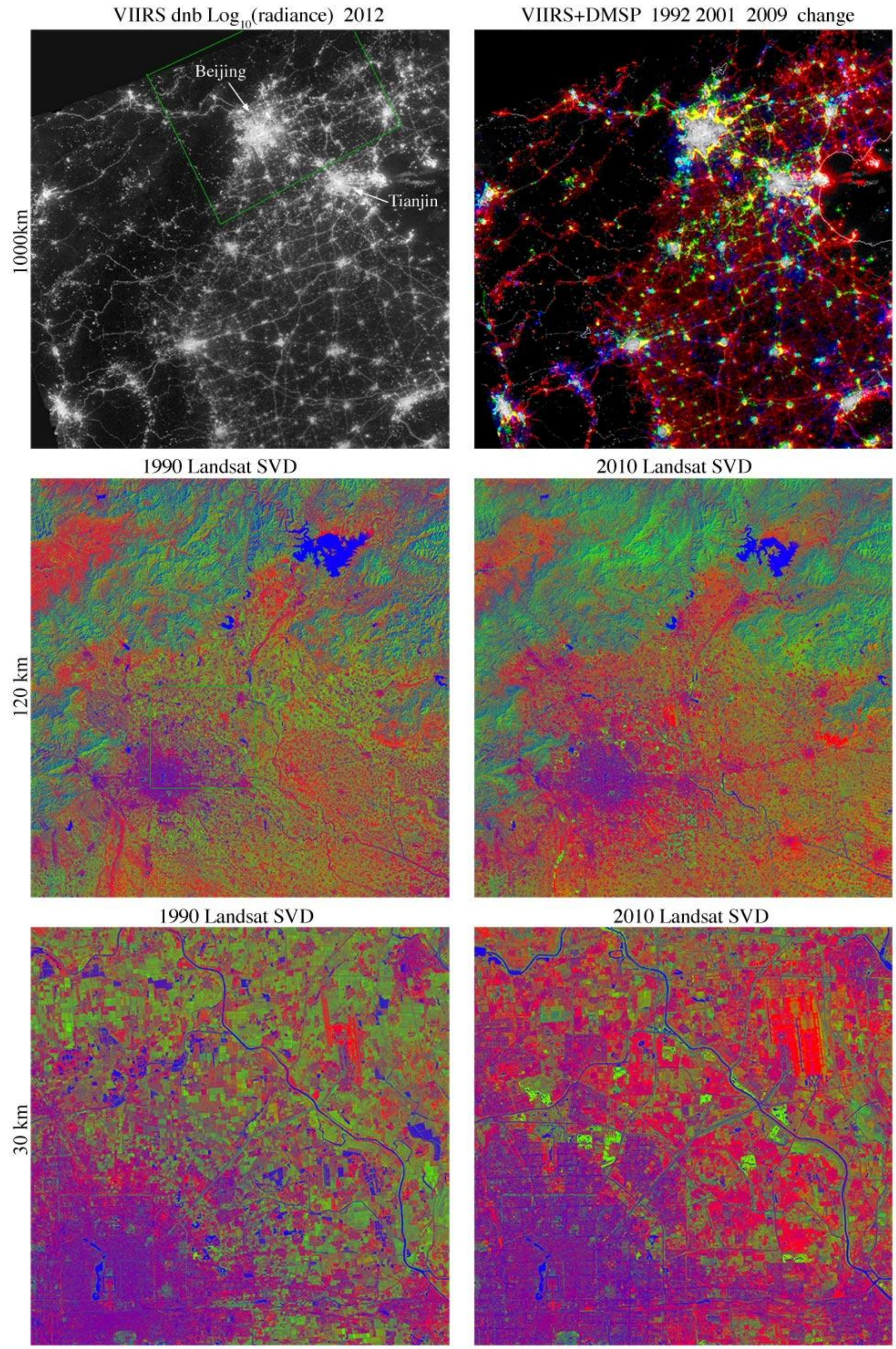

Figure 6 Decadal change of land cover and night light in and near Beijing. Brightening of night lights throughout the North China Plain and surrounding valleys. Earlier brightening (yellow, green) around Beijing, Tianjin and other larger cities in the 1990s was followed by brightening post-2000 of smaller settlements throughout the region. Change of Landsat SVD fractions also shows expansion of shadowed impervious (purple) land cover for settlements of all sizes with pronounced expansion of Beijing. Compared to the other BRIC examples, road networks are much more prominent in VIIRS imagery of China. Most of the road segments show recent brightening (red) but some notable exceptions are green and blue. Within the matrix of brightening, there are several localized areas with pronounced dimming (blue).

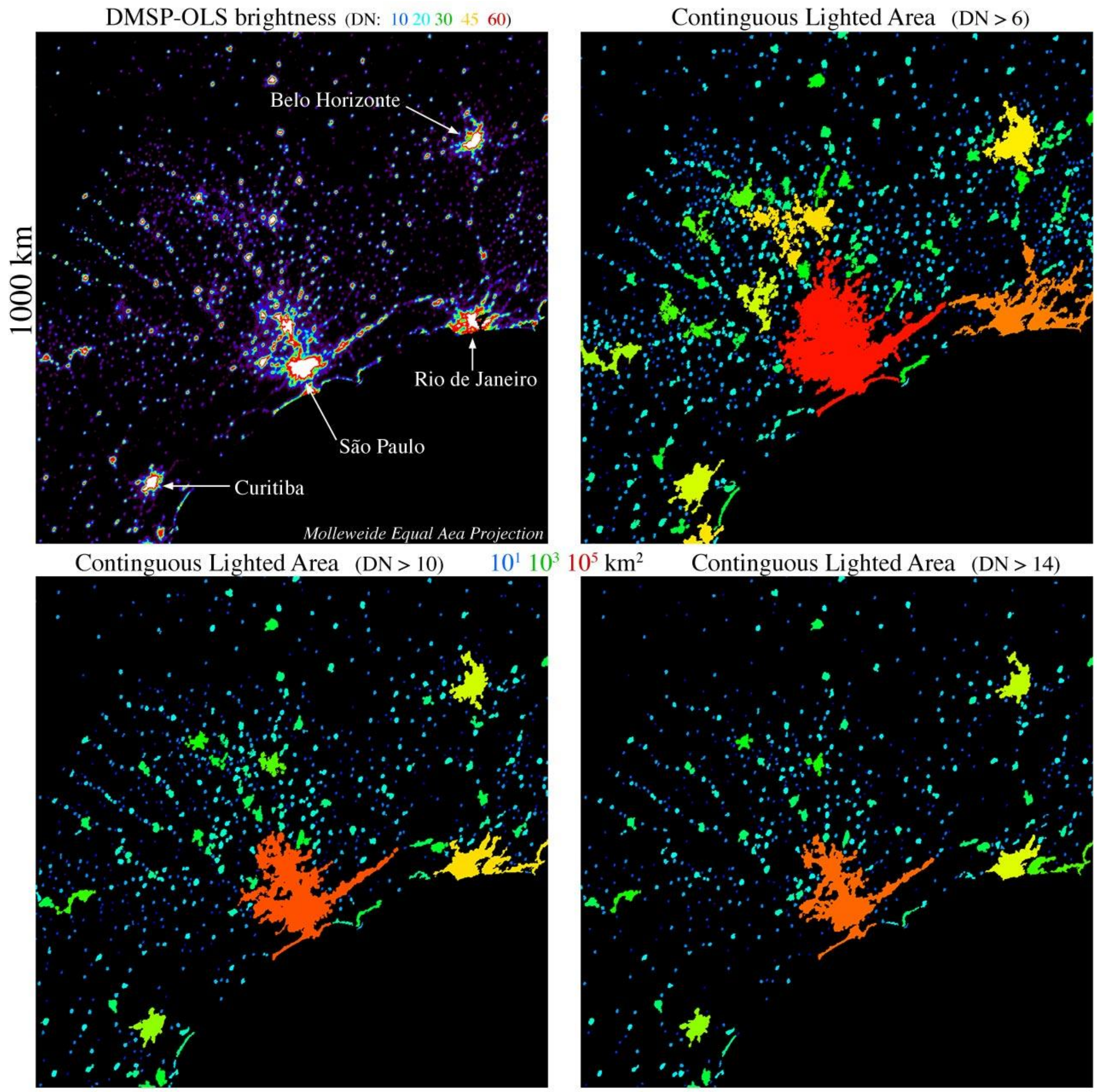

Figure 7 Spatial structure of lighted development and night light brightness around the Southeast Corridor of Brasil. Continuous variation in night light brightness serves as a proxy for varying degrees of development. Bright urban cores saturate the OLS sensor (white areas upper left) but other brightness variations illustrate the tendency for larger settlements to be brighter. Progressive discrete segmention of the continuous brightness field at increasing thresholds results in simultaneous attenuation of smaller light sources and shrinkage of all light sources. In addition to shrinkage and attenuation, larger contiguous segments are fragmented into smaller segments as lower luminance areas connecting brighter areas are attenuated. Fragmentation and shrinkage are the reverse of the analogous processes of urban growth and network evolution.

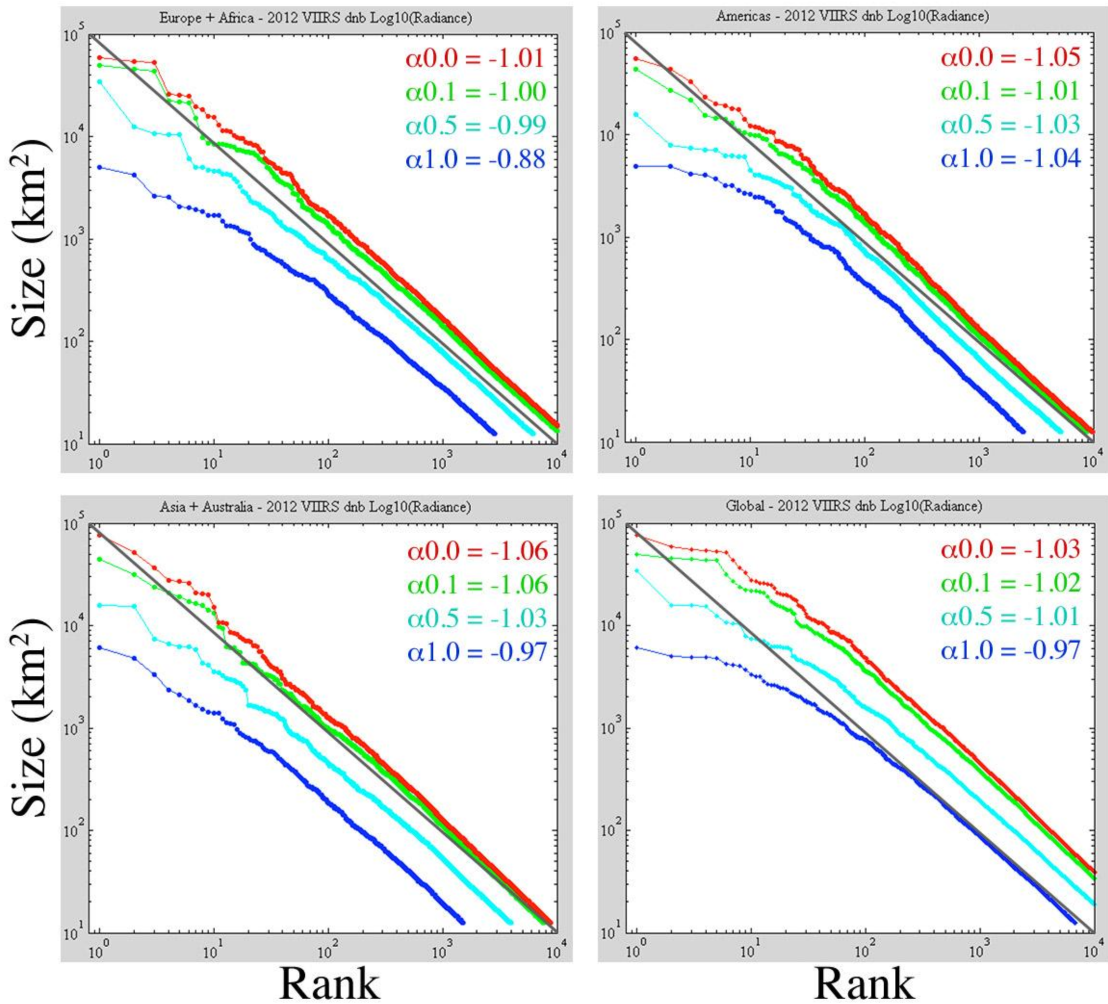

Figure 8 Rank-size distributions of lighted areas in 2012 from VIIRS dnb. Longitudinal sectors of Log_{10}(radiance) are segmented at 4 brightness thresholds for each sector between 10^0 and 10^1 radiance units. The lower threshold corresponds to the point where background noise exceeds anthropogenic signal. The upper threshold corresponds to the point where anthropogenic signal is attenuated. Within this range of thresholds, the best-fit exponent spans -1 for the central (Europe + Africa + Middle East) and eastern (Asia) sectors and for the global distribution - but not for the western (Americas) sector. All distributions except the central a =1.0 have exponents within 0.06 of -1 for all thresholds. Despite the near unity slopes of the lower tail of all distributions, the upper tails of most distributions fall below the 1:1 line - indicating that the largest segments are somewhat smaller than predicted by the power law. The larger segments are much larger than even the largest of individual cities. They represent vast spatial networks of lighted development - although smaller than expected if the process were strictly determined by the power law relationship between rank and size. Nonetheless, the tendency of the distribution to maintain a near-unity slope over 3 orders of magnitude in number and area of segments suggests a persistence of structure that transcends size.

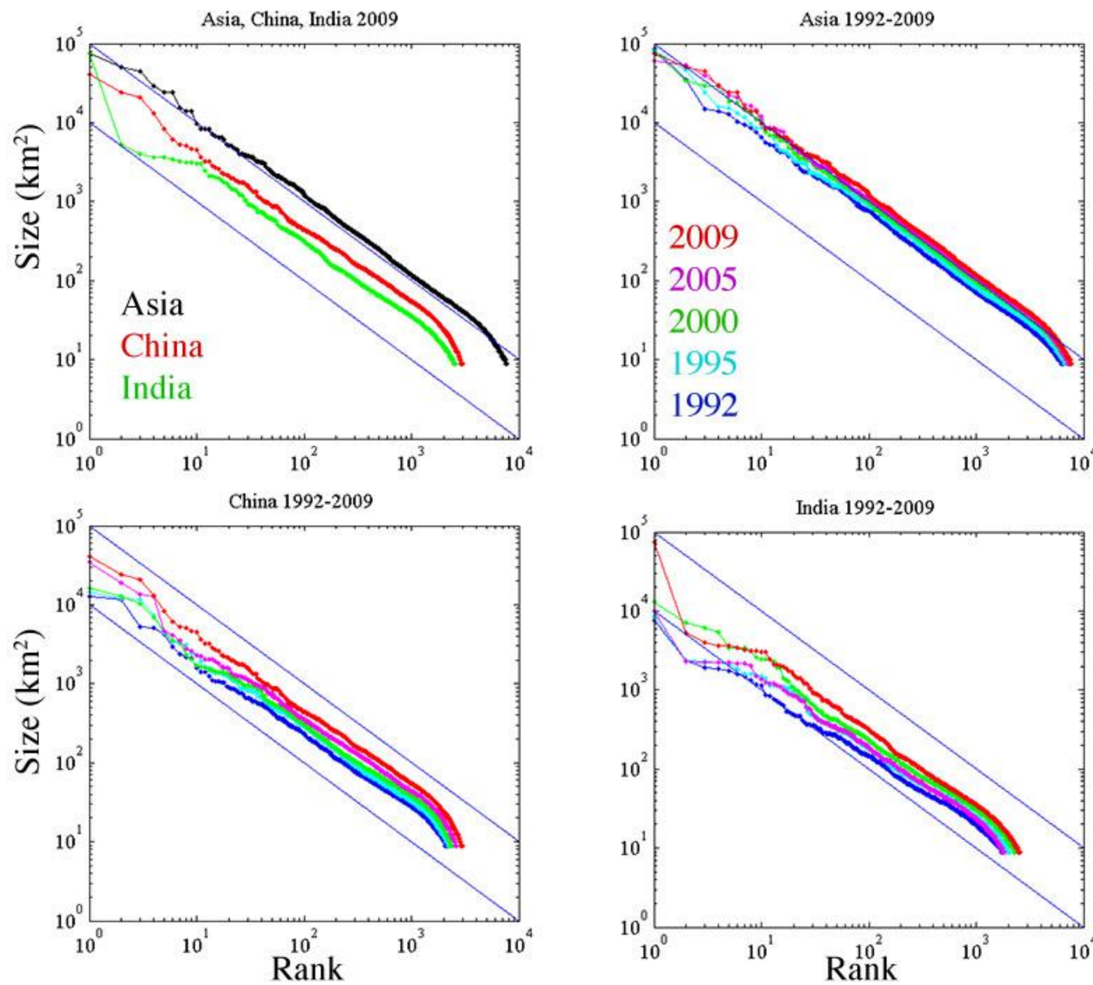

Figure 9 Rank-size distributions in time and space. Each rank-size plot shows the size distribution of all spatially contiguous segments of OLS pixels brighter than11 DN from Small and Elvidge (2013). All slopes but one lie within 0.15 of -1.0 (thin blue lines). Overall, Asia shows stable growth (slope) but India and China both increase slope from 1992 to 2009 as growth increases spatial connectedness and larger agglomerations. Compared to the 2012 VIIRS rank-size distributions, these OLS distributions span a wider range of slopes above and below -1 but their upper tails conform more closely to the predicted linear trend. For India, the persistent disparity between the largest segment and the next 5 to 10 smaller segments represents the dominance of the Punjab region extending north and west from New Delhi. The size of this large network of lighted development is underrepresented on this plot because the part of the network extends into Pakistan is not included. The progressive change of both the overall slope and upper tail of the distributions for China reflect both the widespread growth and development throughout China and the evolution of the largest spatial networks of development. All of these changes contribute to the evolution of the distributions for Asia overall - although the effects are less apparent than in the distributions of China and India alone.